Commonwealth Edison
One First National Plaza, Chicago, Illinois
Address Reply to: Post Office Box 767
Chicago, Illinois 60690

August 24, 1984

Mr. Harold R. Denton, Director
Office of Nuclear Reactor Regulation
U.S. Nuclear Regulatory Commission
Washington, DC 20555

Subject: Dresden Station Units 2 and 3
Quad Cities Station Units 1 and 2
Response to Questions Concerning
Mark I Containment Plant Unique Analysis
NRC Docket Nos. 50-237/249 and 50-254/265

References (a): D. M. Crutchfield letter to D. L. Farrar dated February 14, 1984.

(b): B. Rybak letter to H. R. Denton dated March 29, 1984.

(c): D. M. Crutchfield letter to D. L. Farrar dated July 13, 1984.

Dear Mr. Denton:

References (a) and (c) requested additional information concerning the Mark I Plant Unique Analysis Reports for both Dresden and Quad Cities Stations. The first set of responses were transmitted in Reference (b). The purpose of this letter is to transmit our response to the second and final set of questions. This set of responses was formally presented to members of your staff and their contractors in a meeting held on August 9 and 10. This submittal is consistent with the material presented at that meeting. Attachment A responds to the first nine questions; Attachment B to the tenth and final question.

If you have any questions regarding this submittal, please contact this office.

One signed original and sixty (60) copies of this letter and its attachments are provided.

Very truly yours,

B. Rybak

B. Rybak
Nuclear Licensing Adminstrator

lm

Attachments

cc: R. Bevan - NRR
R. Gilbert - NRR
NRC Resident Inspector - Quad Cities
NRC Resident Inspector - Dresden
B. Segel - NRR (2x)

A025
1/60



9078N

ATTACHMENT A

Dresden Station Units 2 and 3

Quad Cities Station Units 1 and 2

Response to NRC Questions 1 through 9

on the Mark I Plant Unique

Analysis Report

9078N

ITEM 1:

Acceleration volumes for structures with sharp corners such as I-beams are computed on the basis of values in Table 1-4.1-1 for pool swell, C.O., chugging and SRV loadings (Sections 1.4.1.5, 1.4.1.6, 1.4.1.7.3, 1.4.1.8.3 and 1.4.2.4). The stated use of Table 1-4.1-1 is clearly not possible directly as the shapes and flow directions presented do not match any realistic model of some structures such as the ring girder. For Segments 7, 8, 9 and 10 of the ring girder (Table 2-2.2-9 in the Dresden PUAR and Table 2-2.2-11 in the Quad Cities PUAR) give the specific formulas and values of the acceleration volumes for loads in the direction normal to the flange and normal to the web. For post-chug loads shown in Table 2-2.2-9 of Dresden and Table 2-2.2-11 of Quad Cities, identify the chugging downcomers and the phasing relationship and give the local acceleration components at Segments 7, 8, 9 and 10 of the ring girder due to unit source strengths.

RESPONSE TO ITEM 1:

Figures 1-1 and 1-2 show the actual geometry of the ring girders and the models used to calculate the acceleration volumes for the

in-plane and out-of-plane (normal to the web) for Dresden and Quad Cities.

For the in-plane direction (normal to the flange) the ring girders were modeled as I-beams and the formula used to develop the acceleration volumes (Table 1-4.1-1 or K.T. Patton, reference 1-6.0-11. is Quad Cities and Dresden PUARs) for Segments 7 through 10 is:

$$V = [2.11 \pi a^2 + 2c (2a + b-c)] L A_w$$

where

| Parameter | Dresden Value | Quad Cities Value |
|---|---|---|
| a (ft) | 0.625 | 0.334 |
| b (ft) | 1.584 | 1.750 |
| c (ft) | 0.104 | 0.125 |
| L (ft) | 2.739 | 2.739 |
| $A_w$ | 2.0 | 2.0 |
| V ($ft^3$) | 17.30 | 7.19 |

The dimensions a, b, and c are shown in Figures 1-1 and 1-2. The distance L is the segment length for Segments 7 through 10; $A_w$ is the factor to account for wall interference effects.

For the out-of-plane direction, the acceleration volumes for the ring girders were based on the hydrodynamic volume (Table 1-4.1-1

or K.T. Patton, reference 1-6.0-11. in Quad Cities and Dresden PUARs) of a rectangle combined with the actual volume. The formula used to develop the acceleration volumes for Segments 7 through 10 is:

$$V_{Dresden} = (1.33 \pi a^2 + (2b-c)\, c + 2ac]\, L\, A_w$$

$$V_{Quad\ Cities} = [1.207 \pi a^2 + (2b-c)\, c + 2ac]\, L\, A_w$$

where

| Parameter | Dresden Value | Quad Cities Value |
|---|---|---|
| a (ft) | 1.584 | 1.750 |
| b (ft) | 0.625 | 0.334 |
| c (ft) | 0.104 | 0.125 |
| L (ft) | 2.739 | 2.739 |
| $A_w$ | 2.0 | 2.0 |
| V ($ft^3$) | 59.89 | 66.38 |

A total of five post chug cases were evaluated using a combination of two of the four closest vents. Figure 1-3 shows the downcomer locations and numbers, as well as the ring girder. The post chug cases analyzed were:

| Downcomers Chugging | Phasing |
|---|---|
| 1 & 3 | In-phase |
| 1 & 3 | Out-of-phase |
| 2 & 3 | In-phase |
| 3 & 4 | In-phase |
| 3 & 4 | Out-of-phase |

These cases were chosen so that the forces in the x,y and z directions, as well as the moment, are maximized.

The applied loads shown in Tables 2-2.2-9 of the Dresden PUAR and Table 2-2.2-11 of the Quad Cities PUAR were calculated using the highest value for each section and for each direction obtained from the post chug cases identified above. Peak values for accelerations due to a unit source strength at Segment 7 of Dresden are:

| Vents | Phasing | Peak Acceleration ($ft/s^2/ft^3/s^2$) X | Y | Z |
|---|---|---|---|---|
| 1 & 3 | In-Phase | ±.9122 | ±.06579 | ±.04269 |
| 1 & 3 | Out-of-Phase | ±.02425 | ±.01043 | ±.2929 |
| 2 & 3 | In-Phase | ±.46533 | ±.3151 | ±.4078 |
| 3 & 4 | In-Phase | ±.4654 | ±.3939 | ±.6090 |
| 3 & 4 | Out-of-Phase | ±.4711 | ±.3177 | ±.3588 |

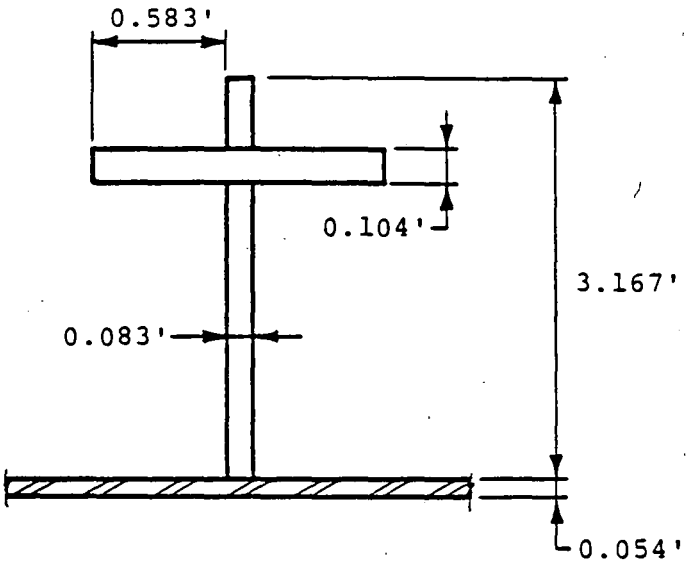


I - ACTUAL GEOMETRY

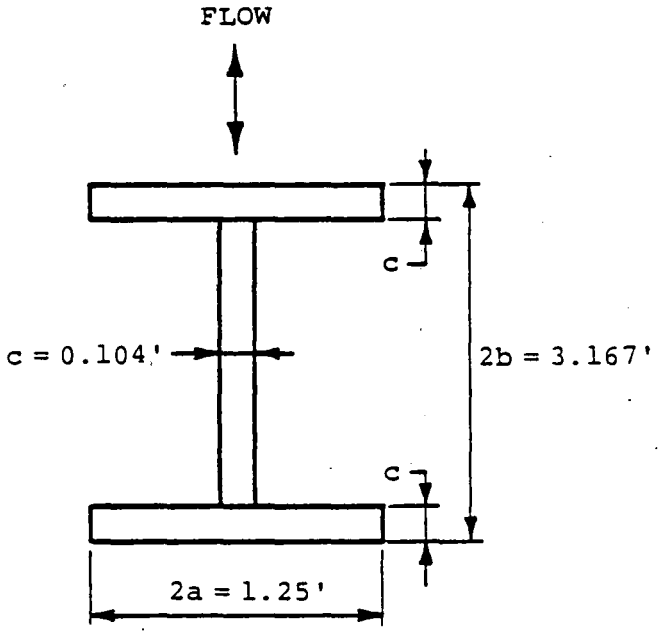


II - MODEL FOR IN-PLANE FLOW

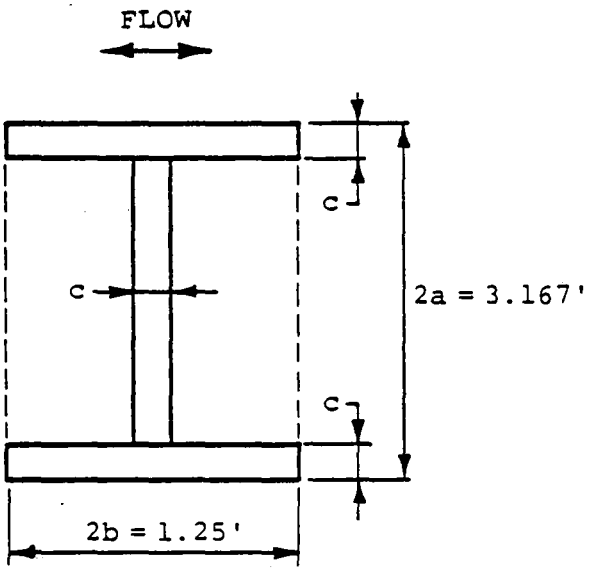


III - MODEL FOR OUT-OF-PLANE FLOW

FCOM84.07-01

Figure 1-1

DRESDEN RING GIRDER

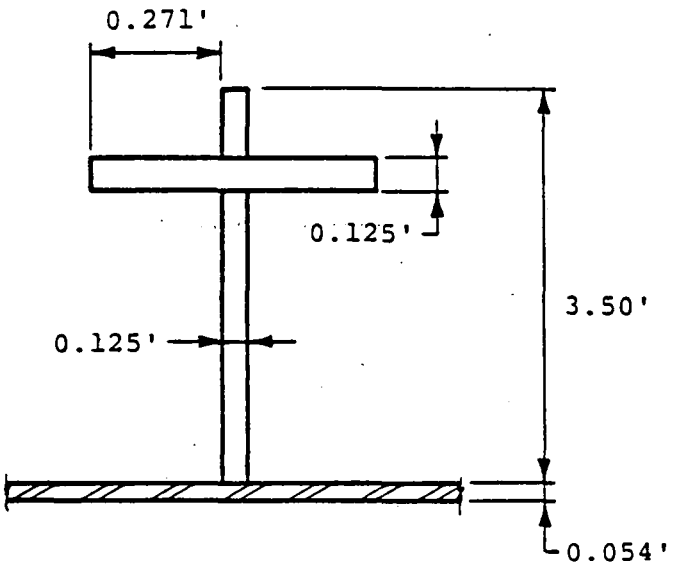


I - ACTUAL GEOMETRY

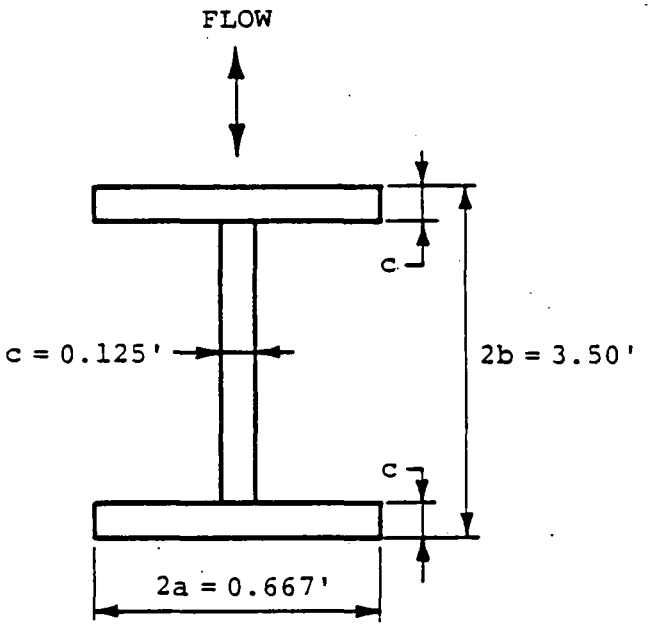


II - MODEL FOR IN-PLANE FLOW

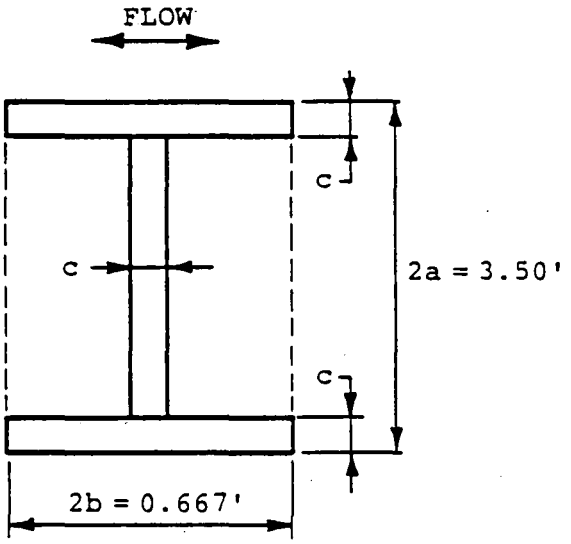


III - MODEL FOR OUT-OF-PLANE FLOW

FCOM84.07-02

Figure 1-2

QUAD CITIES RING GIRDER

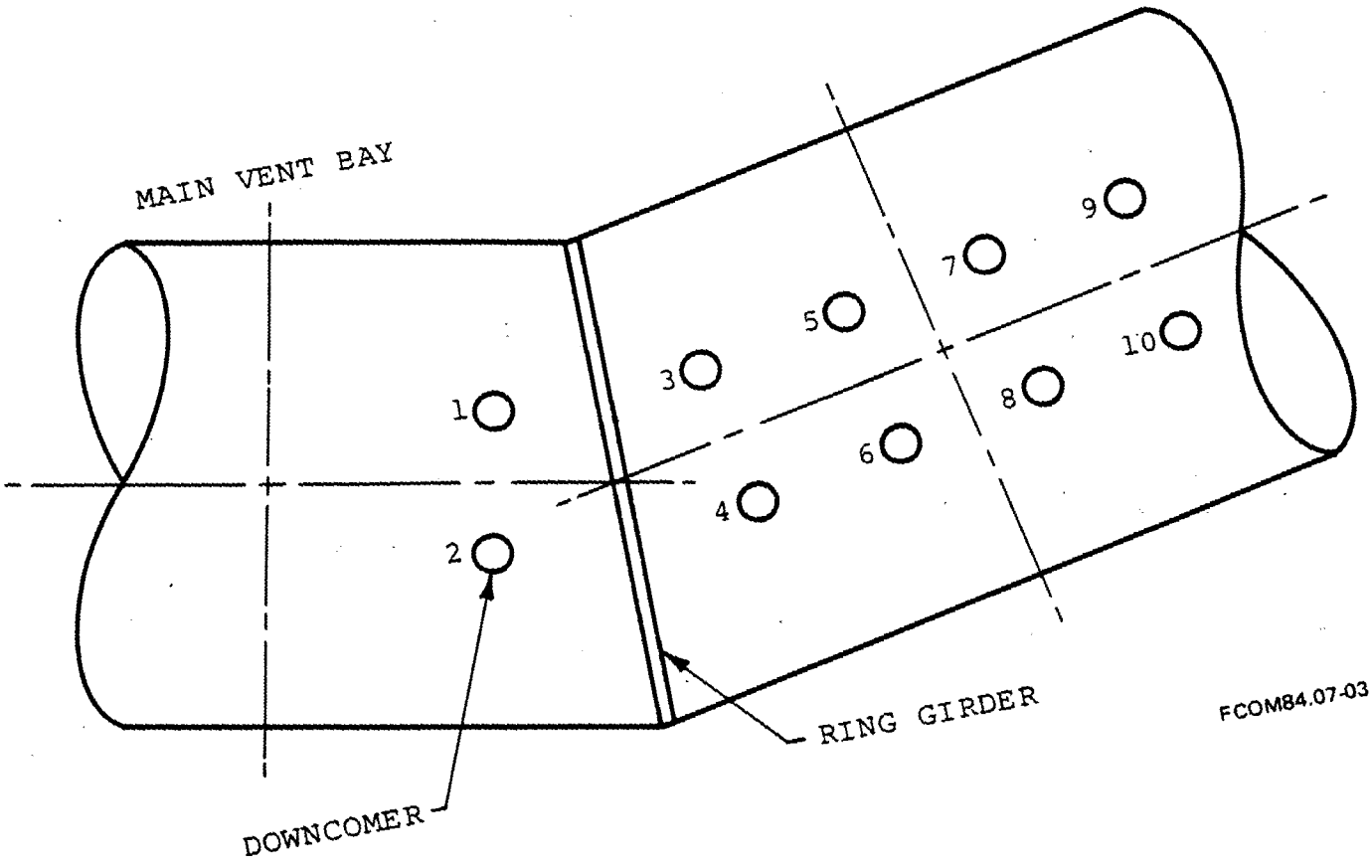


Figure 1-3

DOWNCOMER LOCATIONS

ITEM 2:

Submerged structure loads are applied on the basis of an equivalent static load using Dynamic Load Factors (DLF's). Describe in detail how these DLF's are obtained for the ring girder. Provide information on the critical frequencies and corresponding mode shapes of the ring girder model. If the same DLF's are used for both the flange and web forces, justify this procedure as a conservative interpretation of the real dynamic loading.

RESPONSE TO ITEM 2:

As shown in Figures 2-2.4-1 through 2-2.4-3 in the Quad Cities Plant Unique Analysis Report (PUAR) No. COM-02-039-2 (Revision 0), and Dresden PUAR No. COM-02-041-2 (Revision 0), two finite element models were used to determine critical structural frequencies for the suppression chamber ring girder at each plant. The model shown in Figure 2-2.4-1 was used to determine the in-plane natural frequencies and the modal participation factors shown in PUAR Table 2-2.4-1 required to calculate submerged structure loads on the ring girder flange (mode shapes were not required for this calculation).

The model shown in Figures 2-2.4-2 and 2-2.4-3 was used to determine the out-of-plane natural frequencies and modal participation factors shown in attached Table 2-1 required to calculate submerged structure loads on the ring girder web (mode shapes were not required for this calculation). The dominant in-plane and out-of-plane natural frequencies of 18.87 Hz and 24.87 Hz, respectively, were selected to perform the submerged structure loading analysis for the ring girder.

For condensation oscillation (CO) and chugging (CH) submerged structure loads, these natural frequencies were used to calculate dynamic load factors (DLF) for each of the 50 harmonics defined for these loads in the in-plane and out-of-plane directions. The summation of each DLF times the CO or CH load associated with each of the 50 harmonics was then applied to the finite element models as an equivalent static load.

As defined in the Load Definition Report, safety relief valve (SRV) jet, LOCA bubble drag, and LOCA water jet loads are all conservatively represented by a rectangular step function. The maximum possible DLF for a rectangular step function of 2.0 was used in the analysis.

As discussed in the response to Item 7, a bounding DLF of 2.5 was used in the analysis for SRV bubble drag submerged structure loads.

Table 2-1

RING GIRDER OUT-OF-PLANE FREQUENCY ANALYSIS RESULTS

| Mode Number | Frequency (Hz) | Horizontal Mass Participation Factor (lb.) |
|---|---|---|
| 1 | 24.87 | 7495.8 |
| 2 | 26.46 | 0.0 |
| 3 | 31.32 | 1854.4 |
| 4 | 33.08 | 699.4 |
| 5 | 36.29 | 0.0 |
| 6 | 43.01 | 351.2 |
| 7 | 47.13 | 0.0 |
| 8 | 56.85 | * |

* Note: Mass participation factor not requested for frequencies beyond the load range of 50 Hz.

ITEM 3:

Submerged structure loads require a computation of the velocity and acceleration fields computed on the basis of the method of images applied to a model of the torus bay. Table 1-4.1-2 gives the relevant parameters for the rectangular bay model used for LOCA bubble drag loads. Is the same model used for CO, chugging and SRV loads on submerged structures? If yes, justify the use of this model for structures near the bay boundary (e.g. ring girder, vent header support column) under asymmetric loading conditions, i.e. sources acting in one bay only. If not, describe in detail the models used.

RESPONSE TO ITEM 3:

The rectangular bay model for CO, chugging and SRV loads on submerged structures is similar to that used for LOCA bubble drag loads. As required in Appendix A of NUREG-0661, Model E in NEDE-21983-P is used for the method of images simulation of the torus cross-section for LOCA air bubble, CO, chugging and SRV analyses. The length of the bay model for LOCA air bubble analysis is equal to one actual bay.

Structures may be close to the bay boundary. However, for the CO, chugging and SRV analyses, structures are always placed at or very near the center of the rectangular bay model ($\frac{1}{2}$ D) as shown in Figures 3-1, 3-2, 3-3, and 3-4. From these figures it can be seen that the torus is unwrapped to a length D which is equal to the torus circumference ($D = 2\pi R_{major}$, $D_{Quad\ Cities\ and\ Dresden}$ = 342 ft). Hence, structures are never near the bay boundary and asymmetric loading conditions. Thus, sources acting in one bay only are readily accommodated.

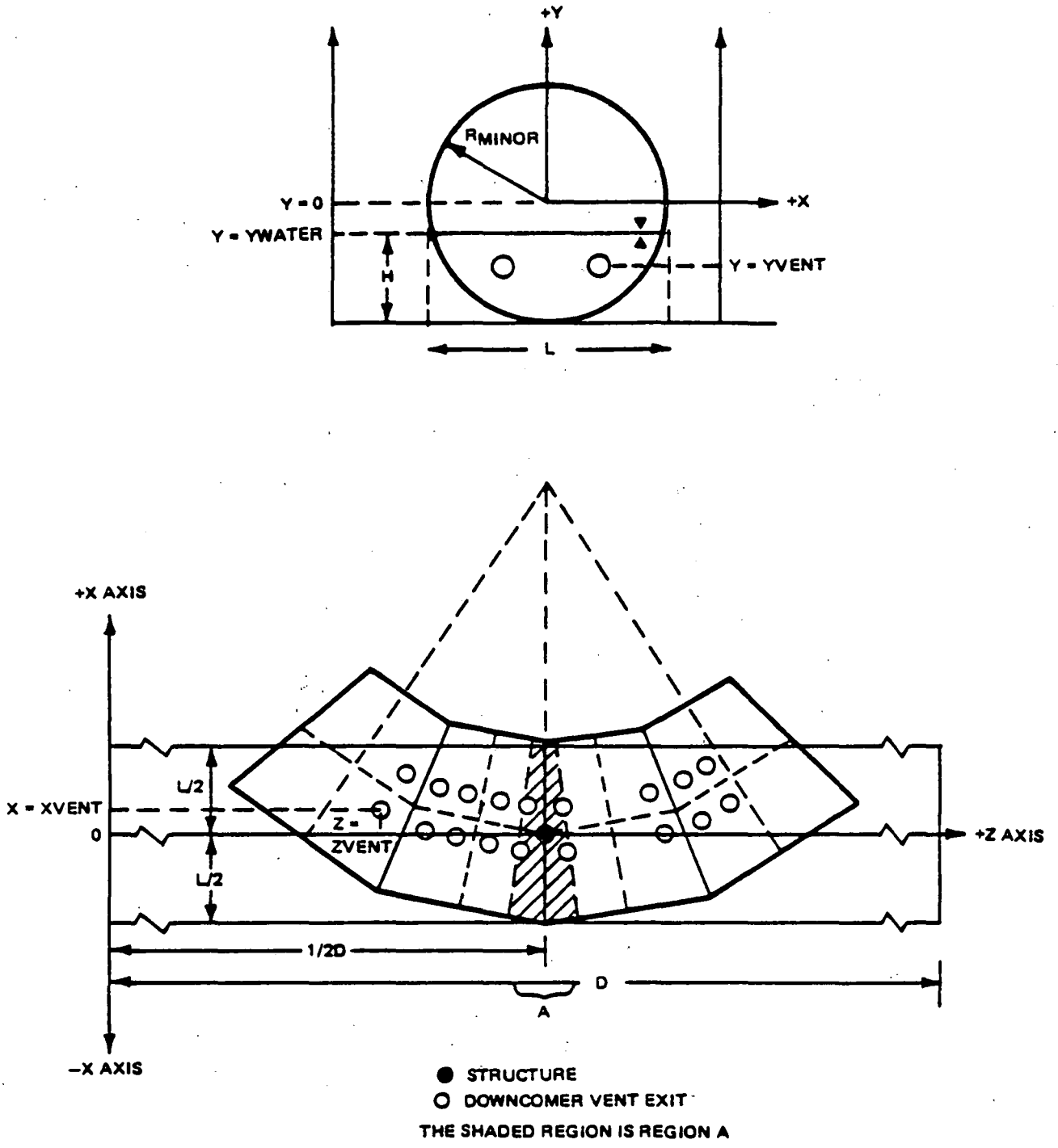


Figure 3-1

RECTANGULAR CELL MODELING FOR PLANTS WITH 96 DCS C.O. AND CHUGGING (CELL A)

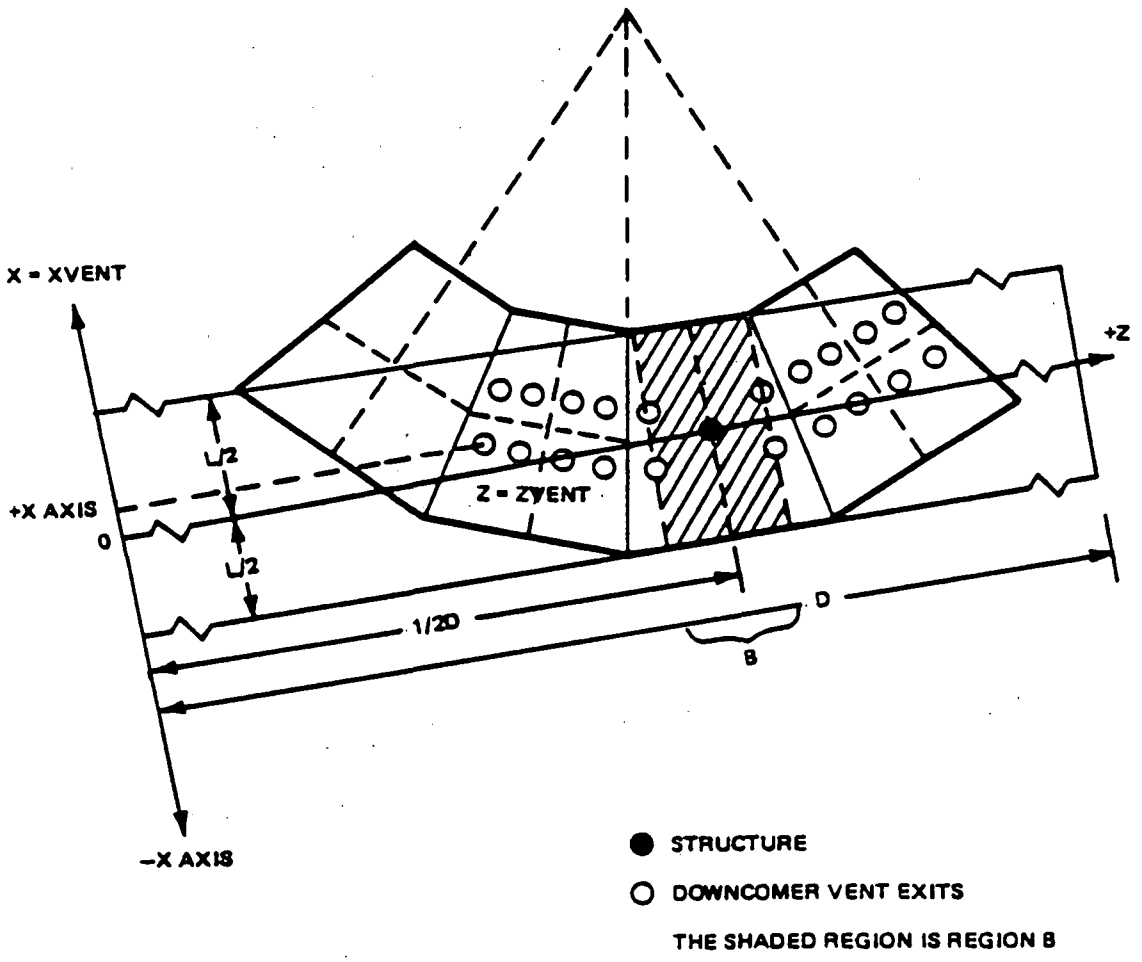


FCOM84.07-05

Figure 3-2

RECTANGULAR CELL MODELING FOR PLANTS WITH 96 DCS C.O. AND CHUGGING (CELL B)

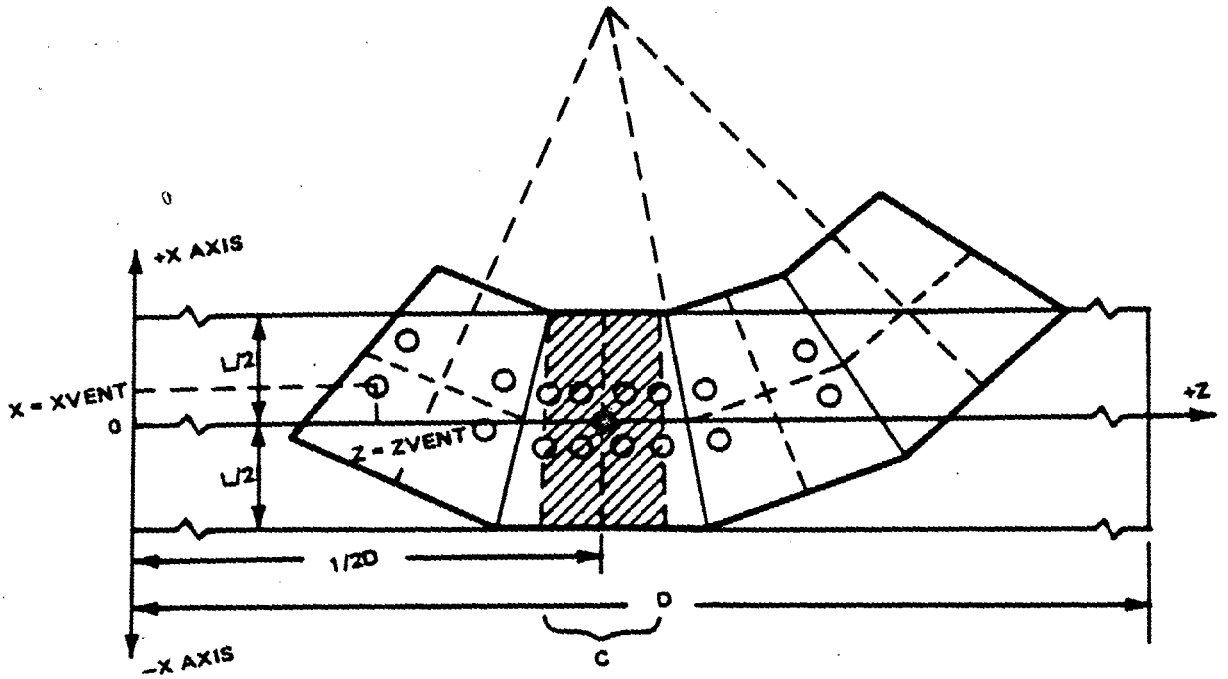


Figure 3-3

RECTANGULAR CELL MODELING FOR PLANTS WITH 96 DCS C.O. AND CHUGGING (CELL C)

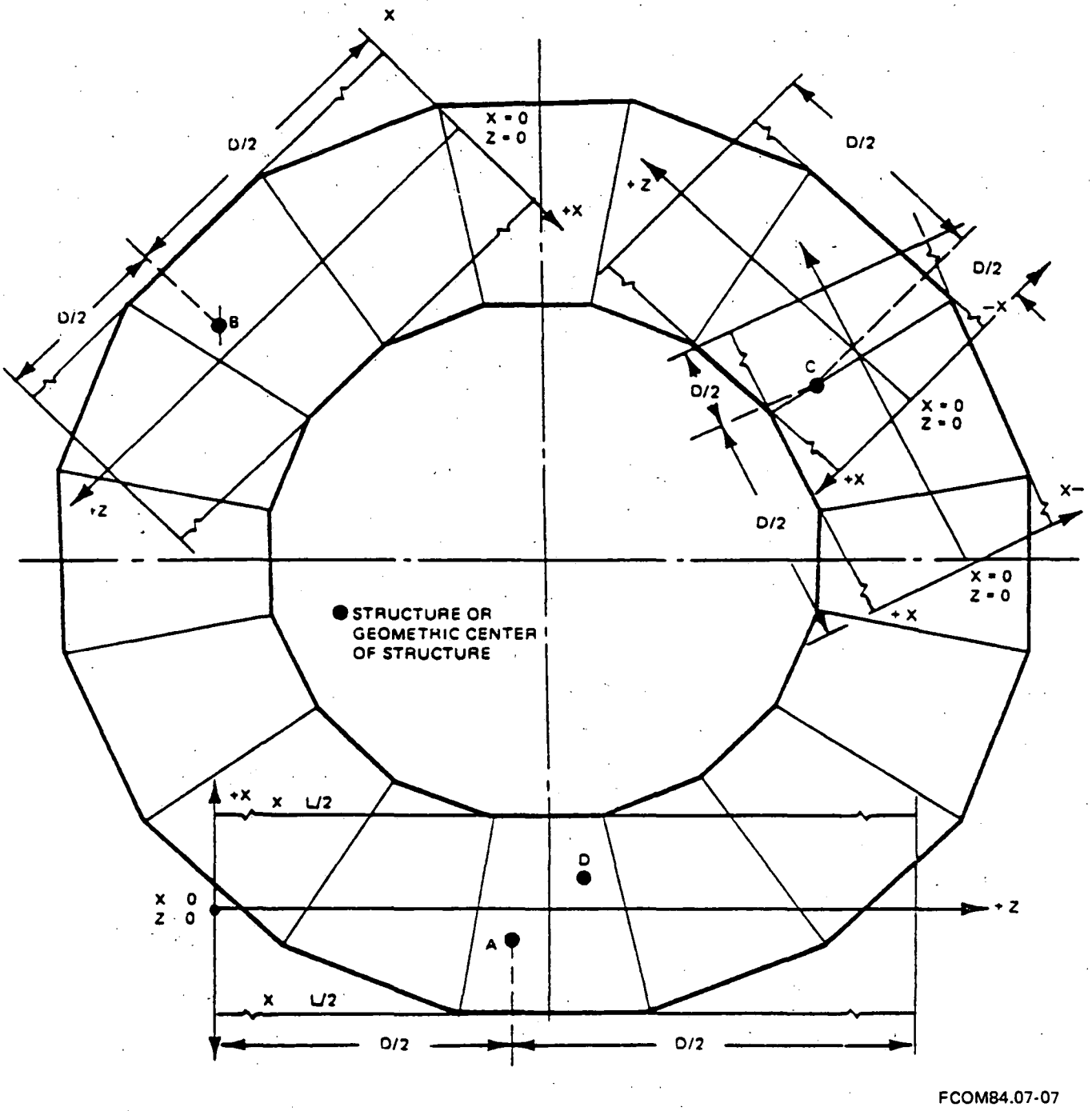


Figure 3-4

RECTANGULAR CELL MODELING -

SRV AIR BUBBLES

ITEM 4:

The PUAR (Section 1.4.1.4.1) states that pool swell impact and drag loads on the main vent-vent header spherical junction are computed according to procedures specified in Appendix A of NUREG-0661. Since no specification is given for spherical structures in Acceptance Criteria, describe which procedure in Appendix A of NUREG-0661 is used and how the spherical junction is modeled.

RESPONSE TO ITEM 4:

The procedure described in Section 2.6 of Appendix A of NUREG-0661 was used to evaluate the pool swell impact and drag loads on the spherical junction for both Quad Cities 1 & 2 and Dresden 2 & 3.

The spherical junction was modeled by a series of cylinders whose axis is along the centerline of the main vent. The spherical junction was subdivided into three equally wide cylinders such that the width is approximately one-third of the diameter, as shown in Figure 4-1. Since the procedure used is that defined for the main vent, the force transient calculated included both acceleration drag and buoyancy. In addition, the velocity drag

was calculated using a conservative value of $C_D$ equal to 2.0, and the projected area of the cylinders, which is larger than that of the sphere.

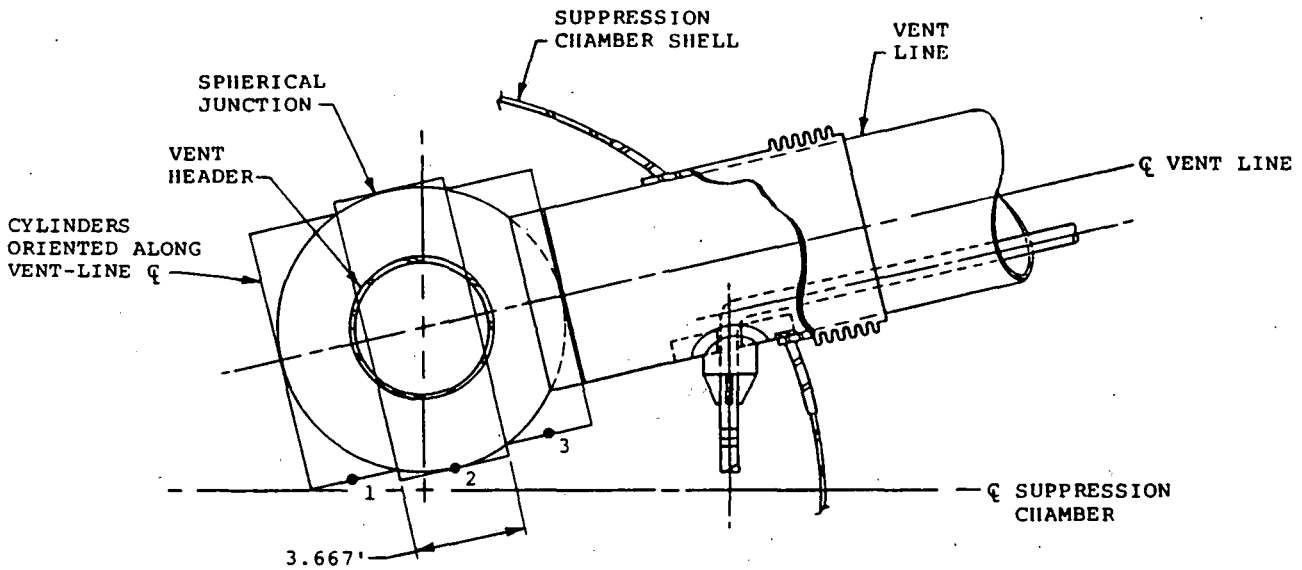


Figure 4-1

SPHERICAL JUNCTION MODELING FOR
POOL SWELL IMPACT AND DRAG

ITEM 5:

The phasing between CO harmonics for torus attached piping is implemented differently than for torus shell loads and for other structures (Section 1.4.1.7.1). Justify this procedure. In particular, explain why a different scale factor is used for Alternate 4 of the CO specification.

RESPONSE TO ITEM 5:

The approach used to combine CO harmonics for torus attached piping is direct summation of the randomly phased harmonics followed by multiplication by a factor of either 1.15 or 1.3. This approach was developed by Dr. Kennedy as part of a generic Mark I program. Dr. Kennedy (SMA) performed a statistical study of CO responses (Reference). From the results of this study it was concluded that a direct summation of the 50 harmonics employing random phasing, multiplied by 1.15, gave a 50% NEP with 90% confidence; a factor of 1.3 gave an 84% NEP with 90% confidence. Dr. Kennedy's study also recommended the 50% NEP value as it gave conservative results which bounded the test data.

In addition to LDR Alternatives 1, 2, and 3 for CO, NUTECH

reviewed the inclusion of a fourth case, Test M-12 by combining the 50 harmonics from Test M-12 with the direct sum method and multiplying by a 1.15 factor. This gave a 50% NEP with 90% confidence factor. These results for M-12 bounded those results for Alternatives 1, 2, and 3 combined with the direct sum method and a 1.3 factor. A factor of 1.3 was used on Load Cases 1, 2, and 3 instead of a 1.15 factor; this introduced some additional conservatism which could be accommodated.

When performing the TAP Plan Unique Analysis for Quad Cities and Dresden, NUTECH utilized the M-12 load case with a 1.15 factor on the direct sum, as it bounded all the test data and the NUREG requirements of Alternates 1, 2, and 3.

Reference: SMA Report 12101.02-R-001D, "Evaluation of Harmonic Phasing for Mark I Torus Shell Condensation Oscillation Loads", dated May 1980.

ITEM 6:

SRV torus shell loads are based on a modified analytical model that is calibrated to bound observed shell pressures in Monticello tests (Section 1-4.2.3). Additional vertical load correction factors are also deduced from Monticello tests. In-plant tests at Dresden Unit 2 are referenced as providing additional confirmation that computed loadings and predicted structural responses are conservative. Provide information on the number of tests performed and the observed maximum shell pressures as well as the predictions of the modified analytical model.

RESPONSE TO ITEM 6:

Attached Table 6-1 presents the test matrix for the Dresden Unit 2 SRV in-plant test. A total of eight tests were conducted for two different sets of initial conditions. Four tests were conducted for first SRV actuation (cold pipe) and four tests for second SRV actuation (hot pipe). The locations of the torus shell pressure transducers are shown in Figures 6-1 and 6-2. Tables 6-2 and 6-3 present the maximum observed and predicted shell pressures for single valve and consecutive valve actuation cases. These tables demonstrate conservatism in the analytical procedure used in generating torus shell loads.

Table 6-1

TEST MATRIX

| Test Number | Test Type | Initial Conditions SRV Pipe | Initial Conditions Pool Temp (°F) | Pipe Cooling Prior to Test |
|---|---|---|---|---|
| SD1 | SD | CP | See Note 1 | |
| MT1 | SVA | CP | | See Note 2 |
| MT2 | CVA | HP | | 1 Min. |
| MT3 | SVA | CP | | See Note 2 |
| MT4 | CVA | HP | | 1 Min. |
| MT5 | SVA | CP | | See Note 2 |
| MT6 | CVA | HP | | 1 Min. |
| MT7 | SVA | CP | | See Note 2 |
| MT8 | CVA | HP | | 1 Min. |

Notes: (1) All tests were run with pool temperature ± 10°F of the starting temperature.
(2) Pipe temperature was within ± 10°F of the temperature before test MT1.

Abbreviations:
SD - Shake Down
SVA - Single Valve Actuation
CVA - Consecutive Valve Actuation
CP - Cold Pipe (SRVDL)
HP - Hot Pipe (SRVDL)
NWL - Normal Water Level (In the SRVDL)

Table 6-2

PEAK PRESSURE LEVELS FOR SINGLE VALVE
DRESDEN IN-PLANT SRV TEST

| Sensor ID | Observed Test Pressures (psi) MT1 | MT3 | MT5 | MT7 | Average | Analytically Predicted Pressures (psi) |
|---|---|---|---|---|---|---|
| P5 | 2.9/-2.0 | 1.5/-2.0 | 2.7/-3.1 | 2.6/-2/7 | 2.4/-2.5 | 4.4/-4.0 |
| P6 | ---- | ---- | ---- | ---- | ---- | 5.1/-4.7 |
| P7 | 2.5/-2.4 | 1.7/-1.8 | 2/0/-2.5 | 2.1/-3.2 | 2.1/-2/5 | 5.7/-5.2 |
| P8 | 2.1/-2.6 | 1.4/-1.5 | 1.9/-2.5 | 2.1/-2.2 | 1.8/-2.2 | 5.7/-5.2 |
| P11 | 2.0/-2.3 | 1.6/-1.5 | 2.0/-2.3 | 2.4/-2.3 | 2.0/-2.4 | 5.7/-5.2 |

Table 6-3

PEAK PRESSURE LEVELS FOR CONSECUTIVE VALVE ACTUATION
DRESDEN IN-PLANT SRV TEST

| Sensor ID | Observed Test Pressures (psi) MT2 | MT4 | MT6 | MT8 | Average | Analytically Predicted Pressures (psi) |
|---|---|---|---|---|---|---|
| P5 | 1.6/-2.5 | 2.2/-1.6 | 1.6/-1.7 | 2.3/-2.4 | 1.9/-2.0 | 5.0/-4.4 |
| P6 | ---- | ---- | ---- | ---- | ---- | 5.8/-5.0 |
| P7 | 1.4/-1.9 | 2.9/-2.0 | 2.3/-2.6 | 1.6/-1.3 | 2.0/-1.9 | 6.4/-5.6 |
| P8 | 1.6/-2.4 | 1.8/-2.5 | 2.2/-2.5 | 2.0/-2.3 | 1.9/-2.4 | 6.4/-5.6 |
| P11 | 1.3/-1.5 | 2.9/-2.2 | 2.5/-2.5 | 1.6/-1.7 | 2.1/-1.9 | 6.4/-5.6 |

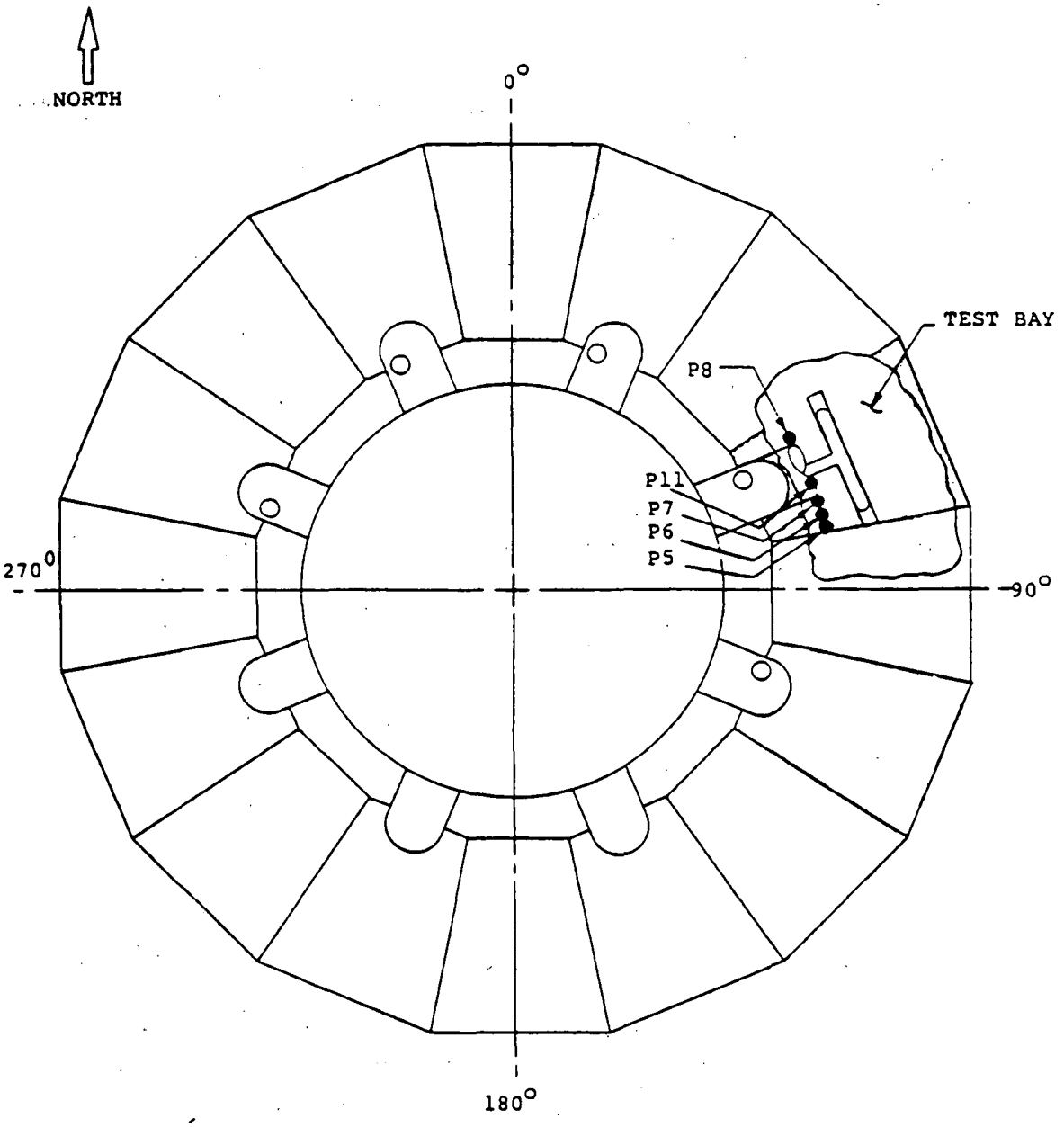


Figure 6-1

PRESSURE TRANSDUCER LOCATIONS IN THE TEST BAY

(PLAN VIEW)

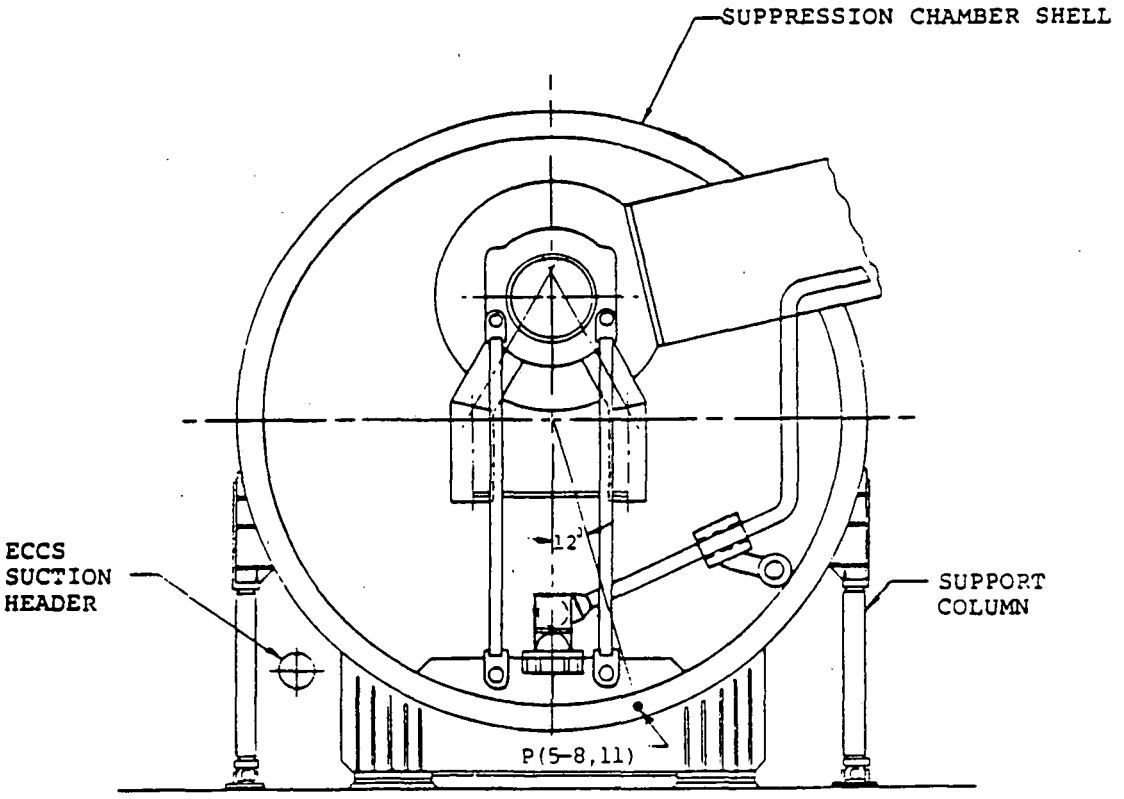


Figure 6-2

PRESSURE TRANSDUCER LOCATIONS IN THE TEST BAY

(ELEVATION)

ITEM 7:

SRV drag loads are computed in accordance with the LDR, but "Dynamic load factors are derived from Dresden's in-plant SRV test data for both Quad Cities and Dresden" (Section 1.4.2.4). Explain exactly how these factors are used and give their numerical values for the major structural components, e.g. for the ring girder and the vent header support column. Describe how test condition information is extrapolated to design conditions, especially those involving multiple valve discharges.

RESPONSE TO ITEM 7:

As permitted by NUREG-0661 (Section 3.10.2.13), Dynamic Load Factors (DLF) for SRV bubble drag submerged structure loads were calculated using SRV discharge bubble pressure time histories measured during the Dresden Unit 2 SRV in-plant test. These bubble pressure time histories were applied to a damped single-degree-of-freedom model. Attached Figure 7-1 is a typical DLF versus structural frequency plot for these pressure time histories.

All submerged structures (e.g., ring girder, vent header support columns, etc.) were analyzed using a bounding DLF of 2.5 times the maximum calculated design bubble pressure loads. The DLF values at resonant condition were developed from the measured pressure-time histories at test conditions and were applied to the design basis event conditions as permitted by NUREG-0661, Section 3.10.2.13.

DYNAMIC LOAD FACTOR VS. STRUCTURAL FREQUENCY
FORCING FUNCTION / TIME HISTORY FOR DRESDEN 2
BUBBLE PRESSURE TIME HISTORY P3-MT7

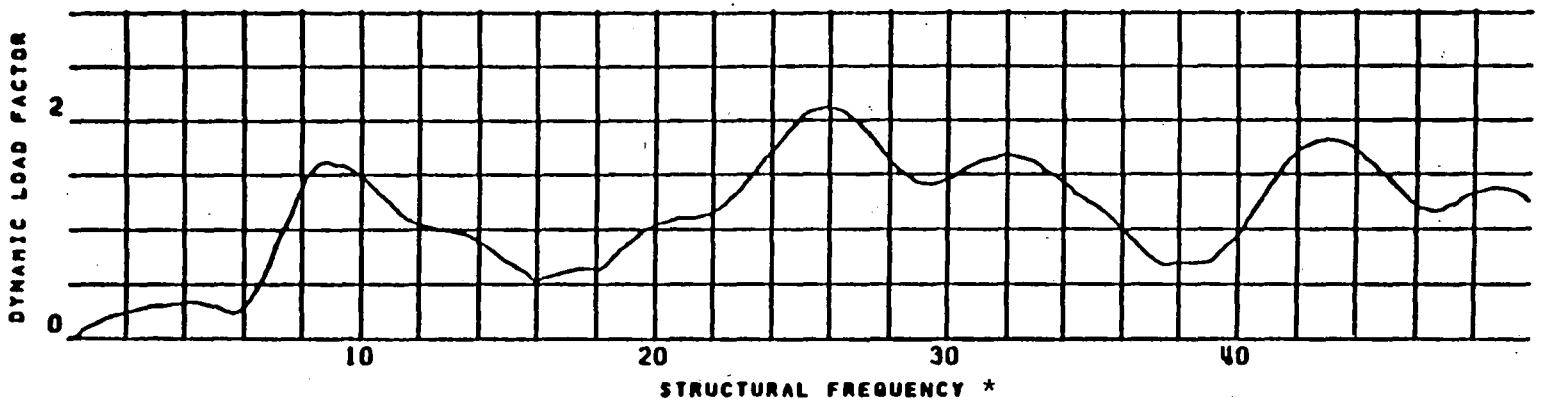


* Hz

Figure 7-1

TYPICAL DLF VS. FREQUENCY PLOT

ITEM 8:

Table 3-2.2-15 of the Dresden PUAR (Table 3-2.2-16 of the Quad Cities PUAR) is inconsistent with Figure 1-4.1-23 of the PUAR. However, the loads as listed in Table 3-2.2-15 (3-2.2-16) are very conservative. Are the loads and downcomer groups as listed in the table(s) the ones used for analysis in Dresden and Quad Cities? Presumably the table heading "Quad Cities Unit 1 & 2 load per Downcomer" of Table 3-2-2-15 of the Dresden PUAR is mislabeled.

RESPONSE TO ITEM 8:

The table and column headings in Dresden PUAR Table 3-2.2-15 are mislabeled. The number of downcomers listed in this table and Quad Cities PUAR Table 3-2.2-16 are also mislabeled. Tables 8-1 and 8-2 present the loads and downcomer groups used in the Dresden and Quad Cities Plant Unique Analyses.

Table 8-1

MULTIPLE DOWNCOMER CHUGGING LOAD MAGNITUDE DETERMINATION

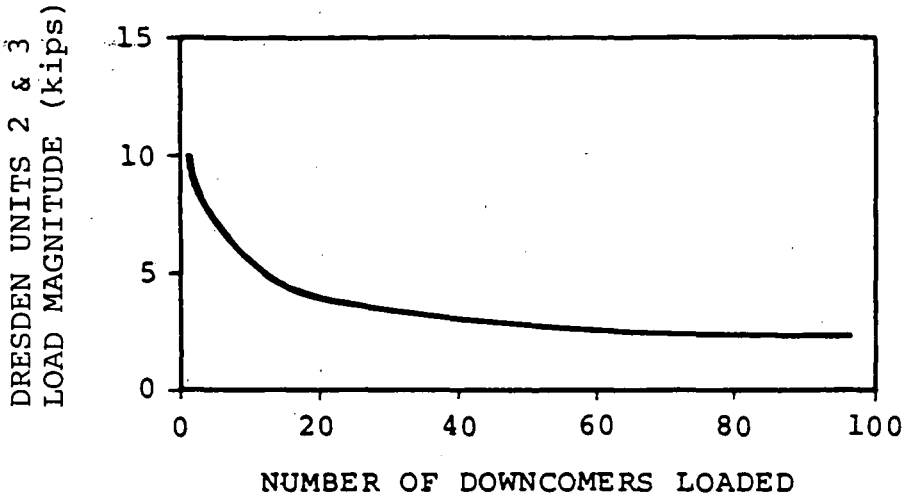


| CHUGGING LOADS FOR MULTIPLE DOWNCOMERS (kips) (1) | | |
|---|---|---|
| NUMBER OF DOWNCOMERS | FSTF LOAD PER DOWNCOMER | DRESDEN UNITS 2&3 LOADS PER DOWNCOMER |
| 1 | 3.05 | 9.75 |
| 5 | 2.10 | 6.75 |
| 10 | 1.42 | 4.54 |
| 20 | 1.00 | 3.20 |
| 40 | 0.72 | 2.30 |
| 80 | 0.58 | 1.86 |
| 120 | 0.54 | 1.73 |

(1) BASED ON PROBABILITY OF EXCEEDANCE OF $10^{-4}$, IN ACCORDANCE WITH NUREG-0661.

Table 8-2

MULTIPLE DOWNCOMER CHUGGING LOAD MAGNITUDE/DETERMINATION

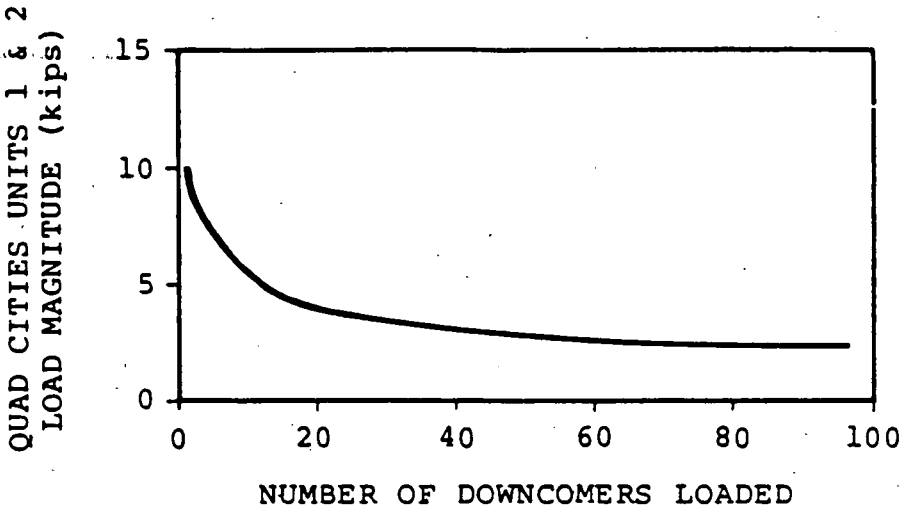


| CHUGGING LOADS FOR MULTIPLE DOWNCOMERS (kips) (1) | | |
|---|---|---|
| NUMBER OF DOWNCOMERS | FSTF LOAD PER DOWNCOMER | QUAD CITIES UNITS 1 & 2 LOAD PER DOWNCOMER |
| 1 | 3.05 | 9.75 |
| 5 | 2.10 | 6.75 |
| 10 | 1.42 | 4.54 |
| 20 | 1.00 | 3.20 |
| 40 | 0.72 | 2.30 |
| 80 | 0.58 | 1.86 |
| 120 | 0.54 | 1.73 |

(1) BASED ON PROBABILITY OF EXCEEDANCE OF $10^{-4}$, IN ACCORDANCE WITH NUREG-0661.

ITEM 9:

Are the entries in Table 3-2.2-3 for $F_1$ and $F_2$ reversed? If not, explain why with the given geometry of the main vent, vertical load components are greater than horizontal ones.

RESPONSE TO ITEM 9:

The entries in Table 3-2.2-3 for $F_1$ and $F_2$ are reversed. However, the loads were correctly applied in the Dresden and Quad Cities Plant Unique Analyses.

ATTACHMENT B

Dresden Station Units 2 and 3

Quad Cities Station Units 1 and 2

Response to NRC Question 10

on the Mark I Plant Unique

Analysis Report

9078N

Item 10:

"In Volume 5 of the PUAR, the statement is made that "one representative SRVDL subsystem was analyzed." Which line was chosen and on what basis was the choice made? Could loads on other lines be higher than on the one analyzed?"

Response to Item 10:

Generally, the SRV discharge lines (SRVDL) are identically routed and supported in the vent pipe area and in the suppression chamber (Torus) for each station. The SRVDL/vent pipe penetration configuration is unique for each station but identical for all SRVDL lines in each unit. Therefore, the submerged structure load analyses and the structural analyses were performed for one SRVDL for each station. Specifically, the piping layout in the suppression chamber and through the vent pipe terminating (cut-point) near the jet deflector at the drywell/vent pipe intersection is identical for all SRVDL of each station. However, the SRVDL routing inside the drywell is unique for each line. To account for the effects of the drywell piping, conservatively chosen spring constants were used in the model to represent the stiffness of the remainder of the drywell piping system.

At the SRVDL cut-point, spring constants were derived from the drywell piping models. The specific drywell model selected was determined by comparing the 10 SRVL's for each station, using analytical isometrics. Line C of Unit 3, for the Dresden model, and Line D of Unit 2 for Quad Cities model, were selected since they were determined to be the most flexible lines. The spring constants for these lines induce the greatest dynamic responses in the SRVDL piping within the vent line and suppression chamber. Therefore, loads on other SRV discharge lines were not expected to be higher than on the lines that were analyzed.